A Fast-Response DC Motor Speed Control System

THADIAPPAN KRISHNAN AND BELLAMKONDA RAMASWAMI

Abstract—**This paper describes the design, construction, and testing of a thyristorized speed control unit for a separately excited dc motor. The motor is fed from a three-phase six-pulse fully controlled thyristor bridge. A speed loop with a proportional plus integral controller maintains the desired speed irrespective of the load variations on the motor. An inner current control loop protects the thyristors from overcurrents. This loop also provides fast response overcoming the effect of disturbances such as variations in supply voltage. The design aspects of the control loops are discussed, and experimental results are given.**

I. INTRODUCTION

IN INDUSTRIES dc motor drives have been widely used for speed control. In the past decades, a motor–generator (Ward–Leonard) set has been used for feeding the dc motor. Nowadays, the thyristor converter has replaced the motor–generator set for well-known reasons [1]–[2]. This article outlines the design aspects of the thyristor converter and the electronic controllers used in closed loop for the speed control of a separately excited dc motor. The salient features of this paper are as follows. 1) At each stage, the system on hand is reduced to a low-order linear system (first, second, or third order, as the case may be) to make the design procedure simple and practicable. The controllers are designed using optimization techniques that have been well tried by engineers. 2) Both transfer functions and step responses are used to characterize the various blocks. 3) All quantities are normalized. The procedure used dispenses with the need to carry through a number of constants and parameters. The normalization also facilitates the simulation of the system on an analog computer.

Section II gives the nomenclature used in this paper. Section III gives the description of the complete system (plant and controllers). In Section IV, various elements of the system are briefly discussed and their transfer functions developed. The design of the current and speed controllers is discussed in Section V. Section VI deals with the experimental results, and Section VII gives conclusions.

II. NOMENCLATURE

Lower case letters represent instantaneous quantities. Capital letters represent parameters, time constants, and base values of normalizing quantities. Capital letters with argument S represent Laplace transforms of normalized quantities. The following is a detailed list of the symbols used.

i_a	Armature current.
I_{st}	Standstill armature current (U_R/R_a).
u_a	Armature voltage.
U_R	Rated armature voltage (220 V).
U_1	Three-phase mains voltage (rms value).
U_2	Secondary voltage of power transformer (rms value).
ω	Motor speed (rad/s).
Ω_0	Motor no-load ideal speed (U_R/K_b).
R_a	Armature resistance.
L_a	Armature inductance.
T_e	Electrical time constant (L_a/R_a).
K_b	Back EMF constant.
K_T	Torque constant ($K_b = K_T$).
J	Moment of inertia of motor and load.
T_m	Mechanical time constant ($J\Omega_0/M_{st}$).
B	Normalized viscous friction constant (includes load on the motor).
m_i	Torque developed by motor.
m_L	Load torque.
M_{st}	Standstill torque (K_bI_{st}).
v_{c1}	Output voltage of current controller.
v_{c2}	Output voltage of speed controller.
V_{cm}	Maximum control voltage (15 V).
v_R	Speed reference voltage.
A	Normalized gain of thyristor amplifier.
v_i	Current transducer output voltage.
H_i	Normalized gain of current transducer.
v_ω	Speed feedback voltage.
H_ω	Normalized gain of speed transducer.
$\mathcal{L}[\cdot]$	Laplace transform of $[\cdot]$.
$I_a(s)$	$= \mathcal{L}[i_a/I_{st}]$.
$U_a(s)$	$= \mathcal{L}[u_a/U_R]$.
$\Omega(s)$	$= \mathcal{L}[\omega/\Omega_0]$.
$M_L(s)$	$= \mathcal{L}[m_L/M_{st}]$.
$V_{c1}(s)$	$= \mathcal{L}[v_{c1}/V_{cm}]$.
$V_{c2}(s)$	$= \mathcal{L}\left[\frac{v_{c2}}{V_{cm}}\right]$.
$V_R(s)$	$= \mathcal{L}[v_R/V_{cm}]$.

III. DESCRIPTION OF SYSTEM

Fig. 1 gives a block diagram of the complete speed control system. A separately excited dc motor driving an alternator is the plant the speed of which is to be controlled. The armature of the dc motor is fed from a three-phase six-pulse fully controlled thyristor bridge. Six tran-

Paper TOD-72-79, approved by the Industrial Control Committee of the IEEE Industry Applications Society for publication in this TRANSACTIONS. Manuscript released for publication April 22, 1974.

The authors are with the Department of Electrical Engineering, Indian Institute of Technology, Madras, India.

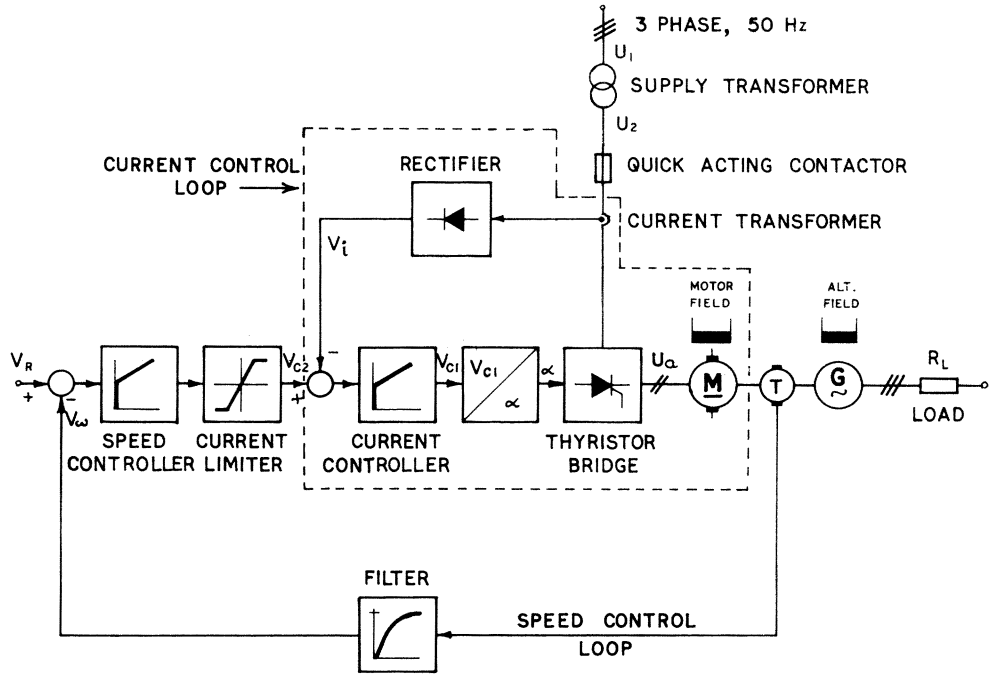

Fig. 1. Schematic diagram of speed control setup.

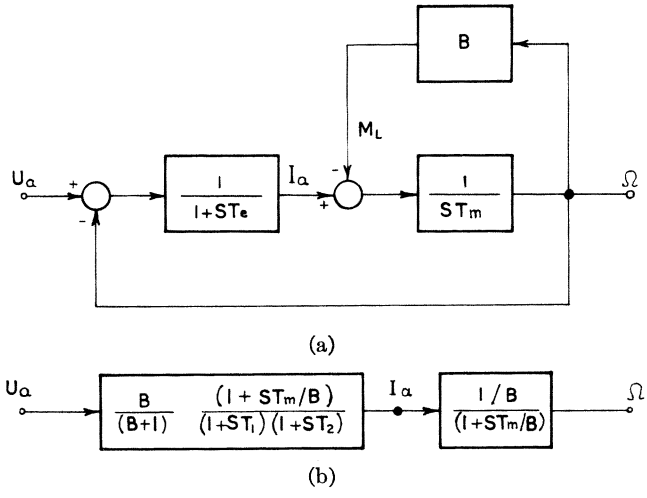

Fig. 2. (a) Block diagram of dc motor. (b) Reduced block diagram of dc motor.

sistorized firing units are used for firing the thyristors, and the firing angle α is controlled by v_{c1}, the output voltage of the current controller. The armature current is sensed on the ac side of the thyristor bridge by means of current transformers and diode rectifiers. The speed is sensed by means of a tachogenerator mounted on the motor shaft.

There are two proportional plus integral (PI) electronic controllers, one the current controller and the other the speed controller designed suitably for providing a fast response. The saturation inherent in the speed controller is used for providing the current limiting. In operation, the speed controller automatically sets the current reference such that the desired speed is maintained independent of the load on the motor.

IV. TRANSFER FUNCTIONS OF VARIOUS ELEMENTS

A. DC Motor

Starting from the differential equations governing the operation of the dc motor, the normalized block diagram of the motor is developed in Appendix I and shown in Fig. 2(a). The ratings of the dc motor used are 220 V, 8.3 A, and 1470 r/min. The pertinent parameters of the dc motor corresponding to the normal operating point (chosen as full load here) are determined as detailed in Appendix II. From Appendix II, the armature time constant $T_e = 18$ ms, the normalized mechanical time constant $T_m = 135$ ms, and the normalized viscous friction constant $B = 0.193$.

The block diagram of the motor given in Fig. 2(a) is reduced to the one shown in Fig. 2(b), where

$$-\frac{1}{T_1}, -\frac{1}{T_2} = \frac{1}{2}\left\{-\left(\frac{B}{T_m}+\frac{1}{T_e}\right) \pm \left[\left(\frac{B}{T_m}+\frac{1}{T_e}\right)^2 - \frac{4(B+1)}{T_m T_e}\right]^{1/2}\right\}. \quad (1)$$

Substituting the values of B, T_m, and T_e given earlier

$$T_1 = 95 \quad \text{ms} \qquad T_2 = 21.5 \quad \text{ms}. \quad (2)$$

B. Thyristor Bridge and Firing Unit

The three-phase six-pulse thyristor bridge used is shown in Fig. 3(a). *RC* circuits to protect the thyristors against hole storage effect [3] are connected in parallel across each thyristor. The quick-acting contactors (operating on thermal and electromagnetic effects) protect the thyristors from any possible overcurrent.

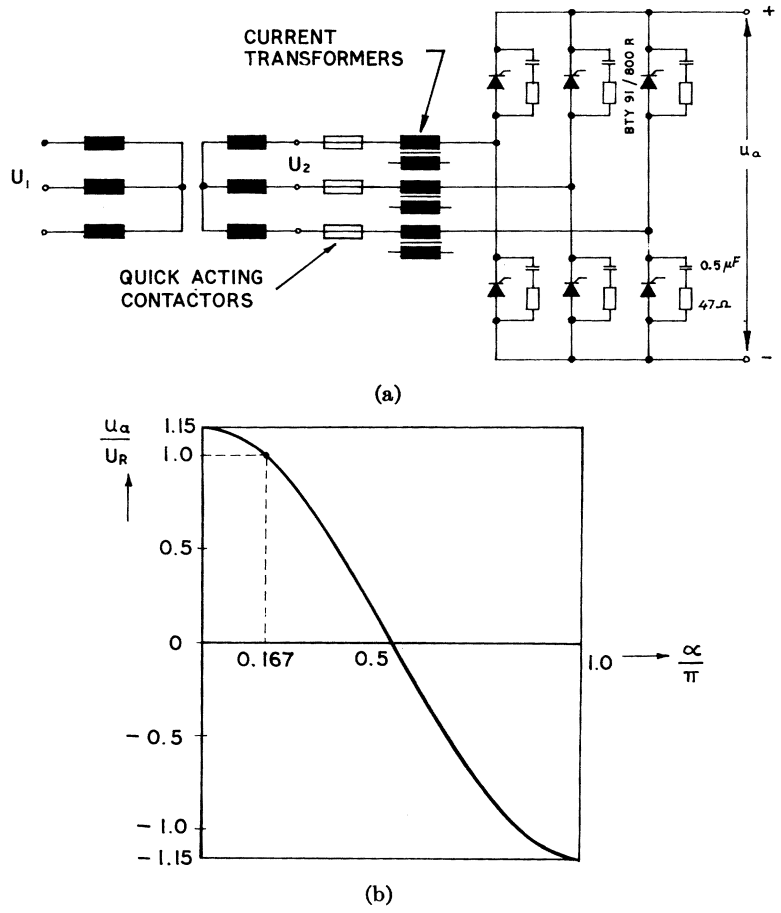

Fig. 3. (a) Thyristor bridge circuit. (b) Thyristor bridge characteristic.

The thyristor converter characteristic is shown in Fig. 3(b). This is a cosine curve, and the gain of the thyristor amplifier changes considerably with the firing angle. It is desirable to operate mainly on the linear part of the characteristic. Therefore, the ac voltage to the thyristor bridge U_2 (secondary voltage of the supply transformer) is chosen such that the rated voltage of 220 V dc is obtained corresponding to a firing angle $\alpha = 30°$. For the converter connection used, the relation between the dc and ac voltages is given by [4]

$$u_a = 1.35U_2 \cos \alpha. \tag{3}$$

Substituting $u_a = 220$ V and $\alpha = 30°$, $U_2 = 188$ V. The gain of the thyristor amplifier is given by $du_a/d\alpha$, and

$$\frac{du_a}{d\alpha} = -1.35U_2 \sin \alpha. \tag{4}$$

Equation (4) is normalized by expressing u_a as a fraction of U_R and α as a fraction of π, the normalizing base for firing angle. Using the values of U_2 and U_R,

$$d(u_a/U_R)/d(\alpha/\pi) = -1.15\pi \sin \alpha. \tag{5}$$

The maximum gain occurs at $\alpha = \pi/2$ and is equal to $-\pi \times 1.15$. The gain at the operating point ($\alpha = \pi/6$) = $-\pi \times 1.15 \times 0.5$. In what follows, the gain of the thyristor amplifier is taken as the average of these two values and is equal to $-\pi \times 1.15 \times 0.75$.

The firing circuit is given in Fig. 4. There are six such units, one for each thyristor. To ensure the self-starting of the thyristor bridge, the pulse output P_{out} of one unit is connected to the other unit at the terminals marked P_{in} in Fig. 4. Due consideration of the phase sequence should of course be taken into account in making these interconnections. The firing unit is so designed and adjusted that the firing angle α varies linearly with the control voltage v_{c1}. The variation of α is from 0 to 180° for a variation of v_{c1} from 0 to -10 V. The gain of the firing unit is α/v_{c1}, and the normalized gain is given by the expression

$$\frac{(\alpha/\pi)}{(v_{c1}/V_{cm})} = \frac{\pi}{-10}\frac{V_{cm}}{\pi} = -1.5. \tag{6}$$

Although the firing angle α is proportional to v_{c1}, the firing of the bridge is not instantaneously corrected. Once the firing pulse occurs, the information in v_{c1} is of no value until the next firing occurs. Hence any system using a thyristor power amplifier should be regarded as a sampled-data system in the strict sense [5]. To make the analysis simpler, the delay in the firing unit is approximated by a simple first-order time lag with a time constant equal to

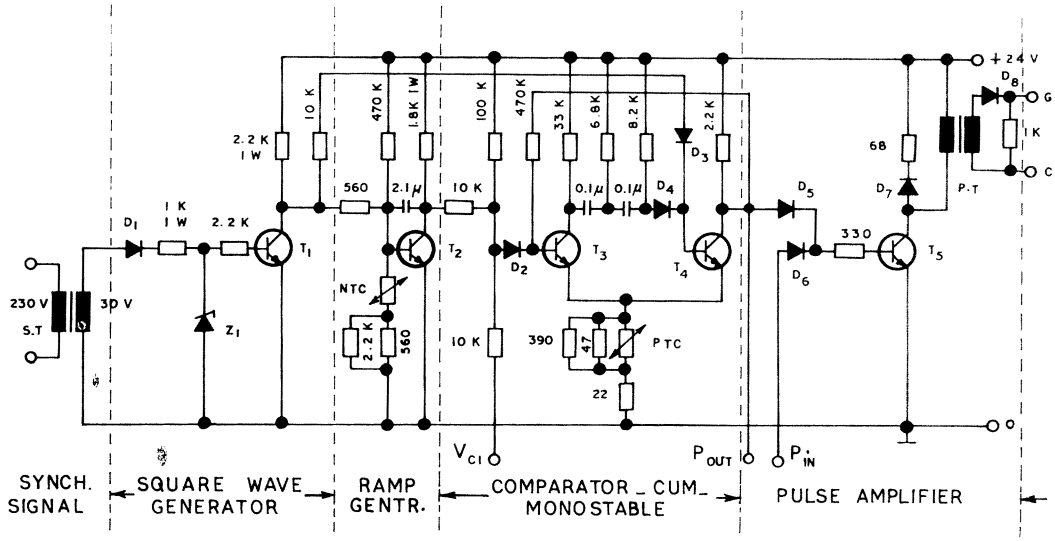

$T_1 \ldots T_4$:	TRANSISTORS	BC 147 A	NTC:	DLY 120
T_5 :	TRANSISTOR	BFX 69 A	PTC:	P/30/50/15/01/ VALVO
Z_1	ZENER DIODE	SZ 111	P.T :	PULSE TRANSFORMER
$D_1 \ldots D_6$:	DIODES	OA 85		900 TURNS / 400 TURNS
D_7 :	DIODE	BAX 13		FERRITE CORE
			S.T :	SYNCH. TRANSFORMER 230/30V

Fig. 4. Firing circuit.

half the period between consecutive firing pulses (i.e., a time constant of 20/12 ms).

Thus the thyristor power amplifier (consisting of the bridge and the firing unit) is approximated by a linear continuous element although it is a nonlinear sampled-data element in reality. The overall normalized transfer function of the thyristor power amplifier is given by

$$\frac{U_a(S)}{V_{c1}(S)} = \frac{(-\pi \times 1.15 \times 0.75)(-1.5)}{(1 + 1.67 \times 10^{-3}S)}$$

$$= \frac{4}{(1 + 1.67 \times 10^{-3}S)} . \quad (7)$$

In the discussion to follow, this transfer function is denoted by $A/(1 + ST_A)$, where $A = 4.0$ and $T_A = 1.67$ ms.

C. Current Control Loop—Current Controller

If the thyristor bridge is under full conduction while starting the motor, the starting current may shoot up to a large value and damage the thyristors. Also, overloads will result in overcurrents. The current control loop shown in Fig. 1 limits the armature current and protects the thyristors from overcurrents. It can be seen from Fig. 1 that the reference for the current control loop is set by the speed controller output. Simply by limiting this quantity, the armature current is also limited to a certain maximum value. The current control loop is suitably designed (see (16) and (17)) such that this maximum corresponds to the permissible maximum current of the motor–thyristor setup.

The current control loop also provides fast response overcoming the effects of disturbances such as variations in supply voltage. How fast response is achieved with changes in supply voltage is now explained assuming that the supply voltage falls. A similar reasoning holds good for an increase in the supply voltage.

Since the electrical time constant T_e of the armature is small compared to the mechanical time constant, the armature current rather than the speed drops almost instantaneously whenever the supply voltage falls. In the absence of the current loop, the motor decelerates to cope with the load torque. The speed comes back to the original value only after the drop in speed is integrated out by the speed controller to give a new firing angle. Hence, for the corrective action to take place, a change in speed has to accompany a change in the supply voltage, and the response is poor on account of the large mechanical time constant involved. With the current control loop present, a fall in armature current itself results in a new firing angle and the fall in supply voltage is counteracted by correcting the armature current at a fast rate.

A PI controller has been chosen for current control since this provides quick response with zero steady-state error. The transfer function of this can be written as $K_1(1 + T_{c1}S)/(T_{c1}S)$, and the design of this (i.e., choosing the parameters K_1 and T_{c1}) is considered in Section V-A.

D. Current Transducer

For the operation of the current loop, a current transducer that senses the armature current is required. Isola-

tion of the control circuit from the power circuit is quite essential. A hall-effect current probe or a magnetic amplifier can be used as a current transducer. In the scheme realized, an inexpensive current transducer is used. The current on the ac side of the bridge (rather than the dc current) is sensed by means of three current transformers. Each secondary output is rectified by a full-wave rectifier, and all the three rectifiers are connected in parallel on the dc side. The overall output voltage v_i is a dc voltage proportional to the armature current.

The gain of this current pickup is v_i/i_a and is found to be 0.46 V/A from experiment. The normalized gain H_i is

$$H_i = \frac{v_i/V_{cm}}{i_a/I_{st}} = 1.69. \tag{8}$$

E. Speed Controller and Speed Transducer

The speed control loop is required to provide a zero steady-state error and a fast response. Hence a PI controller has been chosen for speed control also. The transfer function of the controller is $K_2(1 + T_{c2}S)/T_{c2}S$ and the design of this controller is discussed in Section V-*B*.

A tachogenerator mounted on the motor shaft provides the speed feedback signal. The tachogenerator gain v_ω/ω is found to be 0.382 V/rad/s from experiment. The normalized gain of the speed transducer H_ω is given by

$$H_\omega = \frac{v_\omega/V_{cm}}{\omega/\Omega_0} = 4.44. \tag{9}$$

V. DESIGN OF CONTROLLERS

A. Current Controller

From Fig. 2(b) and the controller configuration assumed in Section IV-*C*, the current control loop is obtained as shown in Fig. 5(a). This is a fourth-order system. The loop gain function is

$$GH_i(S) = \frac{K_1ABH_i}{T_{c1}(B+1)} \cdot \frac{(1 + T_{c1}S)(1 + ST_m/B)}{S(1 + ST_A)(1 + ST_1)(1 + ST_2)}. \tag{10}$$

Since the time constant T_m/B is very large (700 ms) compared to the time constants T_1 (95 ms), T_2 (21.5 ms), and T_A (1.67 ms), the loop gain function valid in the vicinity of the gain crossover frequency can be approximated as

$$GH_i(S) \simeq K' \frac{(1 + T_{c1}S)}{(1 + ST_1)(1 + ST_2)(1 + ST_A).} \tag{11}$$

where

$$K' = \frac{K_1AH_iT_m}{T_{c1}(B+1)}. \tag{12}$$

It is desirable to arrive at a second-order system by choosing T_{c1} such that it cancels one of the plant poles. The resulting second-order system should have a damping factor of 0.707 (widely accepted by engineers) and a gain K' as large as possible since the accuracy increases with K'. Since $T_A < T_2 < T_1$, the requirement just mentioned would be satisfied when $T_{c1} = T_2$ [6], and the corresponding gain $K' \simeq \frac{1}{2}T_1/T_A$. From (12) and the value of K' just given,

$$K_1 = \frac{1}{2}\left(\frac{T_1}{T_A}\right)\left(\frac{T_2(B+1)}{T_mAH_i}\right) = 0.8. \tag{13}$$

Thus the transfer function of the current controller is

$$\frac{K_1(1 + T_{c1}S)}{T_{c1}S} = \frac{0.8(1 + 21.5 \times 10^{-3}\,S)}{21.5 \times 10^{-3}\,S}. \tag{14}$$

The realization of the current controller is shown in Fig. 5(b). The capacitance in the feedback circuit of the operational amplifier is chosen as $c_i = 0.47\ \mu$F, and from the values of K_1 and T_{c1}

$$R_i = 45.8 \quad \text{k}\Omega \qquad R_{1f} = 57.3 \quad \text{k}\Omega. \tag{15}$$

For a maximum armature current of 20 A, the input resistance R_1 is chosen from the relation

$$\frac{v_{c2,\text{sat}}/V_{cm}}{R_1} = \frac{(20/I_{st}) \times H_i}{R_{1f}} \tag{16}$$

where $v_{c2,\text{sat}} = 13.6$ V is the saturation voltage of the speed controller. Substituting for the other parameters in (16),

$$R_1 = 85 \quad \text{k}\Omega. \tag{17}$$

The output of the current controller is limited so that the firing angle always lies between 0 and 150°, the upper limit of 150° being chosen to make sure of proper commutation of the thyristor bridge in the inverting mode. This limiting is achieved through the use of diodes and a zener diode as shown in Fig. 5(b).

The PI controller of the current loop has the transfer function given by (14). The proportional gain of the controller of Fig. 5(b) for the feedback signal, v_i is R_i/R_{1f}, which is denoted by K_1. Since $R_1 \neq R_{1f}$, the gain for the signal v_{c2} of the feedforward path is different and is equal to R_i/R_1. Hence, with the controller of Fig. 5(b), the block diagram representation of Fig. 5(a) should include a gain of R_{1f}/R_1 in the path of v_{c2} only, to correspond to the physical situation. This block of gain R_{1f}/R_1 is shown in Fig. 6(a).

B. Speed Controller

As mentioned in Section IV-*E*, a PI controller is used for the speed loop. For designing this controller, it is necessary to approximate the current loop by a low-order system. It is shown in Section V-*A* that the current loop is actually a fourth-order system, and it has been approximated by a second-order system for design purposes.

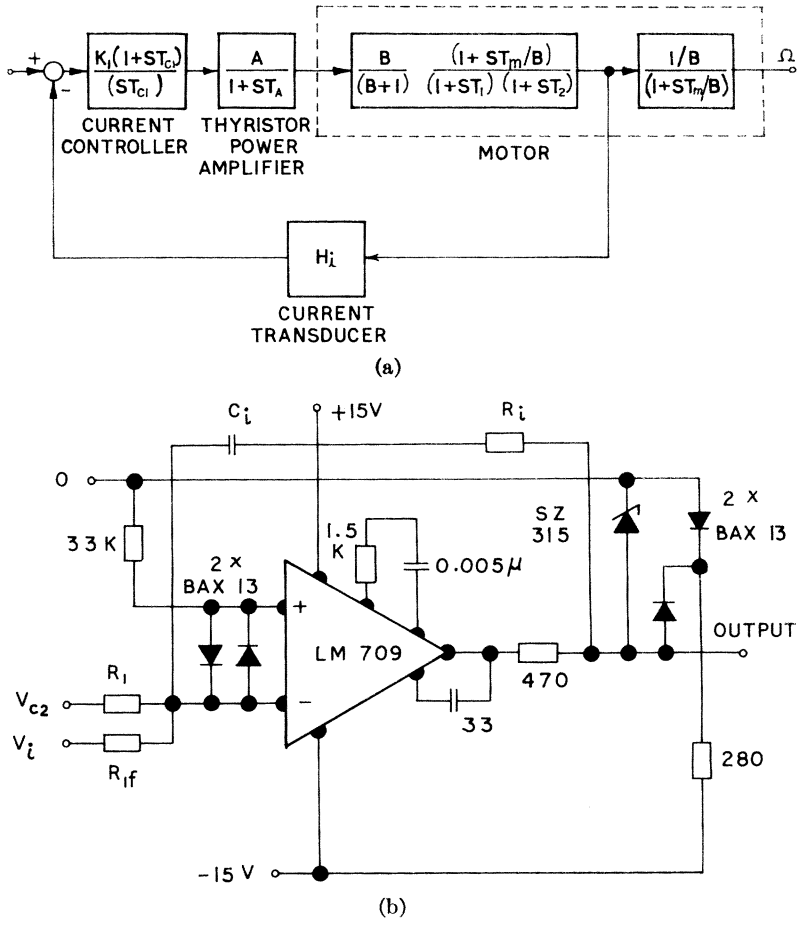

Fig. 5. (a) Current control loop. (b) Current controller.

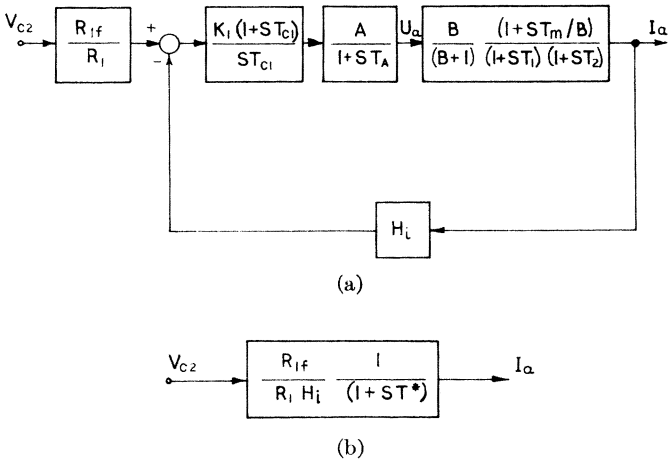

Fig. 6. (a) Actual block diagram of current control loop. (b) Approximated block diagram of (a).

This loop is further approximated by a first-order block of equivalent time constant T^* [6, ch. 15]. This time constant is found to be approximately equal to 10 ms. The approximated current loop transfer function is shown in Fig. 6(b).

The output of the tachogenerator used for sensing the speed signal has a low-frequency ripple of about 25 Hz near the rated speed. Hence an RC filter with a time constant $T_f = 50$ ms is used in the feedback path. The overall block diagram of the speed control loop used for design purposes is shown in Fig. 7(a). The loop gain function is given by

$$GH_\omega(S) = \frac{K_2(1 + T_{c2}S)}{T_{c2}S} \frac{R_{1f}}{R_1 H_i(1 + T^*S)} \cdot \frac{1/B}{(1 + ST_m/B)} \frac{H_\omega}{(1 + ST_f)}. \quad (18)$$

From stability considerations, the controller time constant T_{c2} is to be chosen such that gain crossover occurs at -1 slope, and $1/T_{c2} < \omega_c < 1/T_f$ where ω_c is the gain crossover frequency. Also, the dynamic performance of the loop is largely dependent on the behavior of the loop gain function in the vicinity of ω_c. Based on the numerical values of the time constants involved here, the following approximations can be made in the vicinity of ω_c. 1) The term $1/(1 + ST_m/B)$ can be taken as $1/(ST_m/B)$. 2) The time constant T^* can be neglected. With these approximations, the loop gain function of the speed loop can be simplified as

$$GH_\omega(S) \simeq \frac{(K_2R_{1f}H_\omega)(1 + T_{c2}S)}{(T_{c2}R_1H_iT_m)S^2(1 + ST_f)} \quad (19a)$$

$$= \frac{K_2(1 + T_{c2}S)}{T_{c2}S} \frac{1}{T_lS(1 + ST_f)} \quad (19b)$$

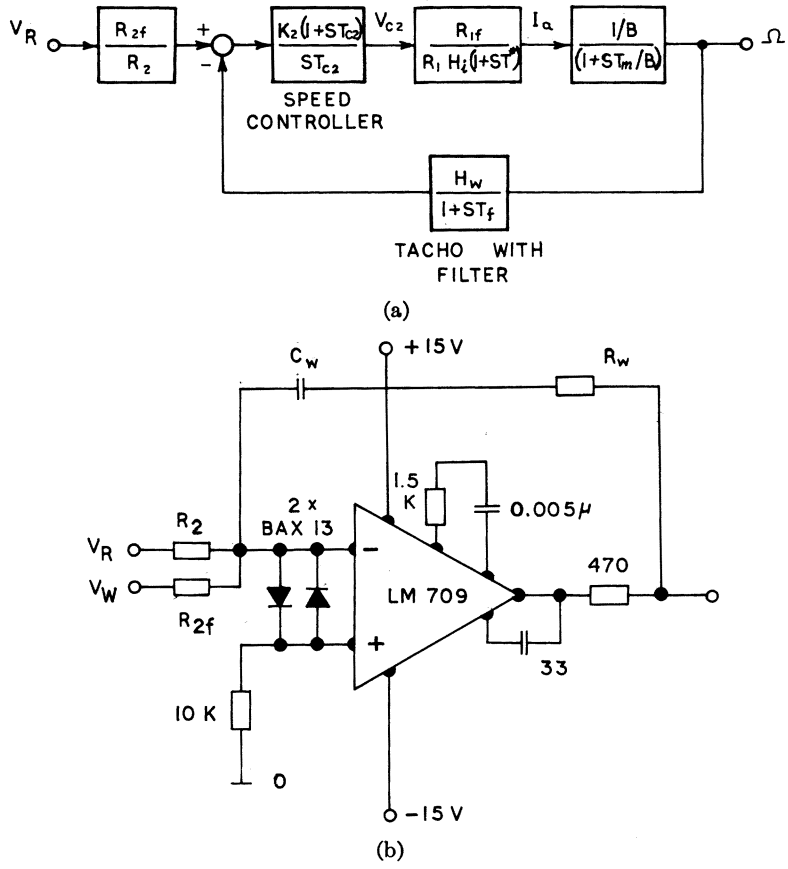

Fig. 7. (a) Speed control loop. (b) Speed controller.

where T_l is the loop integrating time constant. Substituting the numerical values of the parameters

$$T_l = 76.2 \times 10^{-3} S. \tag{20}$$

The PI controller is designed using the symmetric optimum method [6, ch. 13]. This method yields the maximum phase margin for a given ratio of T_{c2}/T_f. The actual ratio of T_{c2}/T_f is chosen such that one of the characteristic roots is real and the other two are complex with a damping of 0.707. The parameters of the controller are given by [6, ch. 13]

$$T_{c2} = (\sqrt{2} + 1)^2 \qquad T_f = 291 \text{ ms} \tag{21}$$

$$K_2 = \frac{1}{(\sqrt{2} + 1)} \qquad T_l/T_f = 0.632. \tag{22}$$

The realization of the controller is shown in Fig. 7(b). The value of the capacitor in the feedback path of the operational amplifier is chosen to be $C_\omega = 1.0\ \mu$F. Using (21) and (22), $R_\omega = 219$ kΩ and $R_{2f} = 460$ kΩ.

The rated speed of the motor is 1470 r/min, and the ideal no-load speed Ω_0 works out to be 1660 r/min. The maximum motor speed Ω_m has been chosen as 1600 r/min, and this should correspond to 15 V, the maximum speed reference voltage. The value of R_2 is accordingly given by

$$\frac{15/V_{cm}}{R_2} = \frac{(\Omega_m/\Omega_0) H_\omega}{R_{2f}} \tag{23}$$

giving $R_2 = 108$ kΩ.

Since $R_2 \neq R_{2f}$, the gain of the controller in Fig. 7(b) is different for the forward and feedback paths. Hence, a block of gain R_{2f}/R_2 should be included in the path of v_R just before the summer so that the block diagram corresponds to the physical situation. The overall transfer function of the speed loop is given by

$$\frac{\Omega(S)}{V_R(S)} = \frac{R_{2f}}{R_2} \frac{G(S)}{1 + G(S)H(S)} \tag{24}$$

where

$$G(S) = \frac{K_2(1 + ST_{c2})}{ST_{c2}} \frac{R_{1f}}{R_1 H_i} \frac{1/B}{(1 + ST_m/B)} \tag{25}$$

and

$$H(S) = H_\omega/(1 + ST_f). \tag{26}$$

Substituting the numerical values and simplifying,

$$\frac{\Omega(S)}{V_R(S)} \simeq \frac{7.96(S + 3.44)(S + 20)}{(S + 8.3)(S^2 + 11.72S + 68.8)}. \tag{27}$$

VI. DISCUSSION OF EXPERIMENTAL RESULTS

A. Current Loop

From Section V-A it can be seen that the compensated current loop is approximated by a second-order system. The analytical values for the time to the first peak T_p and the overshoot M_o can be easily shown to be 10.4 ms

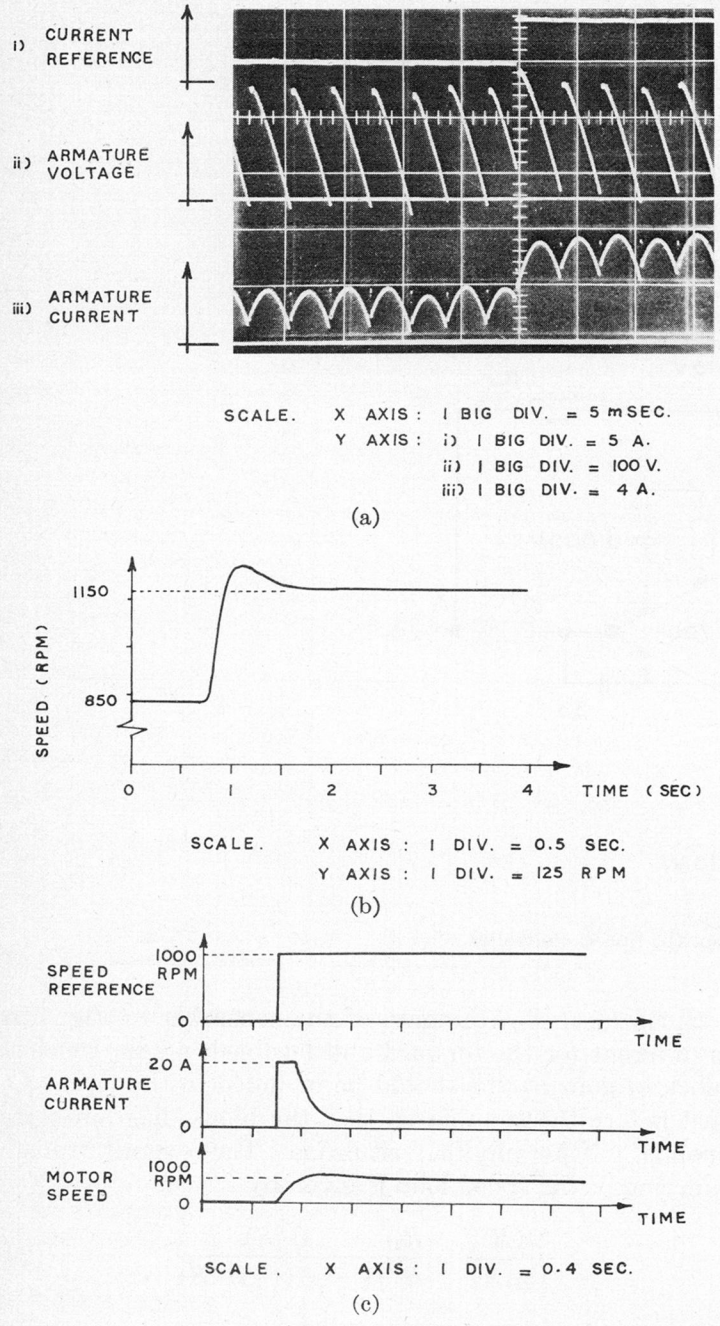

Fig. 8. (a) Current loop response. (b) Speed loop response. (c) Current limiting feature illustrated.

and 4 percent, respectively. Fig. 8(a) shows the photographed response of the current loop (the response is too fast to be recorded with a pen-type recorder). The upper trace of the figure shows the applied current step, the middle trace the manner in which the thyristor output voltage changes, and the bottom trace the armature current. Because of the 300-Hz ripple in the armature current, it is not possible to make out the overshoot, but it can be seen qualitatively that the overshoot is practically negligible.

B. Speed Loop

Equation (27) shows that the speed loop is a third-order system. Analytical values for T_p and M_o are calculated using the method given in [7]. A record of the speed loop response is shown in Fig. 8(b). The analytical and recorded values for T_p and M_o are given in Table I.

TABLE I
RESULTS FOR THE SPEED LOOP

	Analytical	Experimental
T_p	340 ms	350 ms
M_o	32 percent	22 percent

There is a discrepancy of 10 percent in the value for M_o. This can be explained from the fact that the system on hand is actually a nonlinear sampled-data system of at least a sixth order (see (10) and (18)), and the analytical results computed are those for an approximated low-order linear model.

C. Current Limiting

An excellent feature of the scheme described in this paper is the current limiting through the thyristors. Fig. 8(c) illustrates this limiting. The upper portion of this shows the applied speed reference step, the middle one the armature current, and the bottom one the speed. The current limiting can be easily observed from this figure.

VII. CONCLUSIONS

This paper describes a practical speed control system for a dc motor using a thyristor amplifier. Although the actual system is a nonlinear sampled-data one, it is approximated by a low-order linear model. That the approximation is quite good in the engineering sense is demonstrated by the experimental results obtained. Current limiting through the thyristors and the limiting of the firing angle to ensure proper commutation are incorporated in an elegant manner. The inner current loop also provides fast response against disturbances such as variations in supply voltage.

The speed control scheme discussed in this article is useful only for one direction of rotation. Reversal of direction of rotation is a problem quite often come across in industries. With a single thyristor bridge used here, the connections to either the field or the armature could be reversed manually for speed reversal, but this is no solution when automatic control is desired. Two thyristor bridges connected in antiparallel and operated through logic circuits can supply the dc armature current in either direction, and hence the motor can run in either direction without having to reverse the armature connections physically. Work on building up of such a controller operating in a closed-loop manner is in progress in the Control Engineering Laboratory of the Electrical Engineering Department of Indian Institute of Technology, and this will be reported in due course.

APPENDIX I

The differential equations governing the operation of a dc motor with constant field excitation and no mechanical friction are

$$L_a(di_a/dt) + R_a i_a + K_b\omega = u_a \tag{28}$$

$$J(d\omega/dt) = m_i - m_L. \tag{29}$$

The Coulomb and static frictions are neglected for getting a linear model. The viscous friction is not considered here

although it can be adequately taken care of by a linear model. It is included in the load torque m_L. In the experimental setup used, the dc motor is loaded by means of an alternator supplying a resistive load. Neglecting the electrical time constant of the alternator armature circuit, it can be easily shown that the load torque on the dc motor is proportioned to speed. The viscous friction only increases this proportionality constant. For the operating conditions used, this proportionality constant is determined experimentally.

Dividing (28) by U_R ($U_R = R_a I_{st} = K_b \Omega_0$),

$$\frac{L_a}{R_a}\frac{d(i_a/I_{st})}{dt} + \frac{i_a}{I_{st}} + \frac{\omega}{\Omega_0} = \frac{u_a}{U_R}. \tag{30}$$

Taking the Laplace transform of (30) and rearranging the terms,

$$(1 + ST_e) I_a(S) = U_a(S) - \Omega(S). \tag{31}$$

Dividing (29) by M_{st} ($M_{st} = K_b I_{st}$),

$$T_m \frac{d(\omega/\Omega_0)}{dt} = \frac{i_a}{I_{st}} - \frac{m_L}{M_{st}}. \tag{32}$$

Taking the Laplace transform of (32),

$$T_m S\Omega(S) = I_a(S) - M_L(S). \tag{33}$$

The block diagram with normalized quantities shown in Fig. 2(a) is obtained from (31) and (33).

APPENDIX II

The armature resistance R_a is measured by voltmeter–ammeter method and is found to be 4.0 Ω. Keeping the armature blocked, a step of voltage is applied to the armature circuit and the current rise is recorded. From this recording, the electrical time constant T_e is determined as 18 ms. The back EMF constant K_b of the motor is obtained by running the machine as a generator at rated field current and is found to be 1.26 V/rad/s.

The dc machine is loaded by means of an alternator supplying a resistive load. The load torque m_L is proportional to the speed ω, and the proportionality constant B is defined by the equation

$$\frac{m_L}{M_{st}} = B\frac{\omega}{\Omega_0} \tag{34a}$$

that is,

$$M_L(S) = B\Omega(S). \tag{34b}$$

From (33) and (34), the transfer function between Ω and I_a can be written as

$$\frac{\Omega(S)}{I_a(S)} = \frac{1}{B}\frac{1}{(1 + T_m S/B)}. \tag{35}$$

A step armature current is applied to the motor with the alternator loaded, and the speed rise is recorded. From this recording the time constant T_m/B is found as 700 ms. The same test is repeated with the alternator load cut out, and the mechanical time constant T_m is determined as 135 ms. Hence $B = 0.193$.

ACKNOWLEDGMENT

The authors are most grateful to Dr. J. Holtz (formerly with this Institute and currently with Siemens, Erlangen, West Germany) for introducing them to the field of thyristor control of electrical machines. But for the keen interest taken by Dr. Holtz and his help in overcoming several of the practical difficulties encountered, this work would not have been possible. The authors wish to thank Dr. P. Venkata Rao, Head of the Department, for his keen interest and constant encouragement during the progress of the work.

REFERENCES

[1] A. P. Jacobs and G. W. Walsh, "Application considerations for SCR dc drives and associated power systems," *IEEE Trans. Ind. Gen. Appl.*, pp. 396–404, July/Aug. 1968.
[2] K. A. Robinson, "Developed: A standard range of thyristor drives," *Control*, pp. 116–121, Mar. 1964.
[3] G. Irminger, "Thyristor circuitry," *Brown Boveri Rev.*, pp. 657–671, Oct. 1966.
[4] B. D. Bedford and R. G. Hoft, *Principles of Inverter Circuits*. New York: Wiley, 1964, ch. 3.
[5] E. A. Parrish, Jr., and E. S. McVey, "A theoretical model for single phase silicon controlled rectifier systems," *IEEE Trans. Automat. Contr.*, pp. 577–579, Oct. 1967.
[6] W. Leonhard, *Einführung in die Regelungstechnik*. Frankfurt: Akademische Verlagsgesellschaft, Frankfurt, 1969, ch. 11, 13, and 15.
[7] J. J. D'Azzo and C. H. Houpis, *Feedback Control System Analysis and Synthesis*, 2nd Ed. New York: McGraw-Hill, 1966, ch. 8.

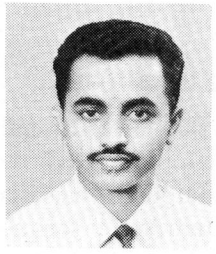

Thadiappan Krishnan was born in Tamil Nadu, India, in 1946. He received B.E.(Hons) degree in electrical engineering in 1968 from the University of Madras, Madras, India, and the M.Tech. in electrical engineering in 1970 from Indian Institute of Technology, Madras.

Since 1970 he has been working as an Associate Lecturer in the Department of Electrical Engineering, Indian Institute of Technology, Madras. He has been doing research and development works in the field of thyristor control of electrical machines.

Bellamkonda Ramaswami was born in Duddukur, India, on September 26, 1934. He received the B.E. degree in 1955 from Andhra University, India, M.S.E.E. degree in 1960 from Purdue University, Lafayette, Ind., and Ph.D. degree in 1967 from the Indian Institute of Technology, Madras, India. He was in the United States under the USAID program and worked as a non-degree student at Purdue University from February 1965 to August 1965 and at Northwestern University, Evanston, Ill., during 1965–1966.

He was a Junior Electrical Engineer with the Andhra Pradesh Electricity Department, India, from 1955 to 1957, where he was involved in the testing of high-voltage metering equipment and protective relays. He served on the faculty at the Engineering College, Kakinada, India, from 1957 to 1959 and at the Indian Institute of Technology, Kharagpur, from October 1960 to June 1961. Since June 1961, he has been on the faculty at the Indian Institute of Technology, Madras, where he is currently an Associate Professor in Electrical Engineering. His research interests include transformer analog computers, linear systems theory, and optimal and suboptimal control systems. Currently he is working in the areas of static power conversion and closed-loop speed control of electrical machines using thyristor power amplifiers.